Gallic Acid Induces G_0/G_1 Phase Arrest and Apoptosis in Human Leukemia HL-60 Cells through Inhibiting Cyclin D and E, and Activating Mitochondria-dependent Pathway

RU-DUAN YEH[1,2], JUNG-CHOU CHEN[1,2], TUNG-YUAN LAI[3], JAI-SING YANG[4], CHUN-SHU YU[5], JO-HUA CHIANG[6], CHI-CHENG LU[6], SU-TSO YANG[3,7], CHIEN-CHIH YU[5], SHU-JEN CHANG[5], HUI-YI LIN[5] and JING-GUNG CHUNG[8,9]

[1]*The School of Chinese Medicine for Post-baccalaureate, I-Shou University, Kaohsiung 824, Taiwan, R.O.C.;*
[2]*Department of Chinese Medicine, E-DA Hospital, Kaohsiung 824, Taiwan, R.O.C.;*
Schools of [3]*Chinese Medicine, and* [5]*Pharmacy, Departments of* [4]*Pharmacology, and*
[9]*Biological Science and Technology, China Medical University, Taichung 404, Taiwan, R.O.C.;*
[6]*Department of Life Sciences, National Chung Hsing University, Taichung 402, Taiwan, R.O.C.;*
[7]*Department of Radiology, China Medical University Hospital,*
China Medical University, Taichung 404, Taiwan, R.O.C.;
[9]*Department of Biotechnology, Asia University, Taichung 413, Taiwan, R.O.C.*

Abstract. *Gallic acid (GA) induces apoptosis in different types of cancer cell lines. In this study, we investigate the apoptotic effects induced by GA in human promyelocytic leukemia HL-60 cells, and clarify the underlying mechanism. Our results showed that GA reduced the viability of HL-60 cells in a dose- and time-dependent manner. GA led to G_0/G_1 phase arrest in HL-60 cells through promoting p21 and p27 and inhibiting the levels of cyclin D and cyclin E. GA caused DNA damage and fragmentation in HL-60 cells as assayed using DAPI staining and Comet assay. Flow cytometric analysis revealed that GA increased Ca^{2+} levels and reduced the mitochondrial membrane potential ($\Delta\Psi_m$) in HL-60 cells. Apoptotic protein expressions were determined by Western blotting. The results indicated that GA-mediated apoptosis of HL-60 cells mainly depended on mitochondrial pathway, by promoting the release of cytochrome c, apoptosis-inducing factor (AIF) and endonuclease G (Endo G) and by up-regulating the protein expression of Bcl-2-associated X protein (BAX), caspase-4, caspase-9 and caspase-3. In addition, GA also activated the death receptor-dependent pathway by enhancing the protein expressions of fatty acid synthase (FAS), FAS ligand (FASL), caspase-8 and BCL-2 interacting domain (BID). We determined the mRNA expression of the gene levels of these proteins by real-time PCR. The results showed that GA-mediated apoptosis of HL-60 cells mainly depended on up-regulation of the mRNA of caspase-8, caspase-9, caspase-3, AIF and Endo G. In conclusion, GA-induced apoptosis occurs through the death receptor and mitochondria-mediated pathways. The evaluation of GA as a potential therapeutic agent for treatment of leukemia seems warranted.*

Correspondence to: Jing-Gung Chung, Department of Biological Science and Technology, China Medical University, No. 91, Hsueh-Shih Road, Taichung 404, Taiwan, R.O.C. Tel: +886 422053366 ext. 2161, Fax: +886 422053764, e-mail: jgchung@mail.cmu.edu.tw

Key Words: Gallic acid (GA), human leukemia HL-60 cells, apoptosis, death receptor-mediated pathways, mitochondria-mediated pathways.

Gallic acid (3,4,5-trihydroxybenzoic acid, GA), an intermediate component of plant (1), has demonstrated antioxidant (2), antibacterial (3), antifungal and antimalarial (4), and antiherpetic action (1). GA was found to induce apoptosis in human leukemia cells (5), lung cancer cell lines (6), stomach cancer cells, colon adenocarcinoma cells (7) and PC12 rat pheochromocytoma cells (8). GA can play an important role in the prevention of malignant transformation (9) and prevents amyloid beta (Aβ)-induced apoptotic neuronal death (10). GA also had antitumor effects on LL-2 (11) and NCI-H460 lung cancer cells both *in vitro* and *in vivo* (6). There is no report to show whether GA affects human leukemia HL-60 cells *in vitro*. In the present study, the effects of GA on the growth and apoptotic cells death of human leukemia HL-60 cells *in vitro* were investigated.

Materials and Methods

Chemicals and reagents. GA, propidium iodide (PI), dimethyl sulfoxide (DMSO), ribonuclease A (RNase A), trypan blue and Triton X-100 were obtained from Sigma-Aldrich Corp. (St. Louis, MO, USA). RPMI-1640 medium, trypsin-EDTA, penicillin-streptomycin,

fetal bovine serum (FBS) and L-glutamine were obtained from Invitrogen by Life Technologies (Carlsbad, CA, USA). The fluorescence probes 2,7-dichlorodihydrofluorescein diacetate (H_2DCFDA), 3,3'-dihexyloxacarbocyanine iodide ($DiOC_6$), Fluo-3/AM and 4,6-diamidino-2-phenylindole dihydrochloride (DAPI) were obtained from Invitrogen.

Cell culture. Human promyelocytic leukemia cell line (HL-60) was obtained from the Food Industry Research and Development Institute (Hsinchu, Taiwan, R.O.C.). Cells were placed into 75-cm^2 tissue culture flasks and maintained at 37˚C under a humidified 5% CO_2 atmosphere in RPMI 1640 medium supplemented with 10% FBS, 100 U/ml penicillin, 100 μg/ml streptomycin and 2 mM L-glutamine.

Assessments of morphological changes and viability in HL-60 cells. Cells were seeded in 24 well plates at a density of 1×10^5 cells/well and grown for 24 h until 80% confluency. Different concentrations (0, 10, 25, 50, 75 and 100 μM) of GA were added to each well and cells were incubated for 24 and 48 h at 37˚C, 5% CO_2 and 95% air. To determine morphological changes and cell viability, the phase-contrast microscopy and a PI exclusion method by using a FACSCalibur utilizing BD CellQuest Pro software (Becton-Dickinson, San Jose, CA, USA) were used as previously described (12-13).

Flow cytometric analysis for DNA content of HL-60 cells. To estimate cell cycle distribution in HL-60 cells, cellular DNA contents were measured by flow cytometry as described elsewhere (14-15). Approximately 2×10^5 cells/well in 24-well plates were treated with different concentrations of GA (0, 10, 25, 50, 75 and 100 μM) for 24 h. After cells were harvested by centrifugation, cells from each treatment were fixed by 70% ethanol in 4˚C overnight and re-suspended in PBS containing 40 μg/ml PI and 100 μg/ml RNase A and 0.1% Triton X-100 in the dark for 30 min at room temperature. The cell cycle distribution was determined and analyzed by flow cytometry as described previously (14, 16).

DAPI staining for determining the apoptotic cells. Cells at a density of 1×10^5 cells/well were plated onto 24-well plates and incubated with different concentrations of GA (0, 10, 25, 50, 100 and 200 μM) for 24 h treatment before being isolated for DAPI staining as described previously (17-18). After staining, the cells were examined and photographed using a fluorescence microscope.

Comet assay for examining DNA damage. Approximately 2×10^5 cells/well in 12-well plates were incubated with GA at final concentrations of 0, 50, 75 and 100 μM, vehicle (1 μl DMSO) and 5 μM of hydrogen peroxide (H_2O_2, positive control) grown for 24 h at 37˚C in 5% CO_2 and 95% air. At the end of incubation, cells were harvested and examined for DNA damage using the Comet assay as previously described (19-20). Comets for PI-stained DNA tails of the individual nucleus in GA-treated HL-60 cells were visualized, measured and photographed by using a fluorescence microscope and were quantified by TriTek Comet Score V 1.5 software (TriTek Crop., Sumerduck, VA, USA) (17, 21).

Detection of the level of mitochondrial membrane potential ($\Delta\Psi_m$), Ca^{2+} production and reactive oxygen species (ROS). Approximately 5×10^5 cells/well were treated with or without 50 μM GA for 0, 3, 6, 12 and 24 h to detect the alterations of $\Delta\Psi m$ and Ca^{2+}. Cells were harvested, re-suspended in 500 μl of $DiOC_6$ (1 μmol/l) and Fluo-3/AM (2.5 μg/ml), respectively (13, 18) and then analyzed by flow cytometry. Untreated cells and cells treated with GA at a concentration of 50 μM for 0.5, 1, 3, 6 and 12 h were stained with H_2DCFDA (10 μM) in 500 μl PBS for analysis of changes in ROS (22). All of the cells were incubated with the fluorescent probes for 30 min at 37˚C in a water-bath and analyzed immediately by flow cytometry as described elsewhere (13, 18, 22).

Table I. *Primer sequences for real-time PCR*.

Primer name	Primer sequence (5'-3')
Caspase-3	F-CAGTGGAGGCCGACTTCTTG
	R-TGGCACAAAGCGACTGGAT
Caspase-8	F-GGATGGCCACTGTGAATAACTG
	R-TCGAGGACATCGCTCTCTCA
Caspase-9	F-TGTCCTACTCTACTTTCCCAGGTTTT
	R-GTGAGCCCACTGCTCAAAGAT
AIF	F-GGGAGGACTACGGCAAAGGT
	R-CTTCCTTGCTATTGGCATTCG
Endo G	F-GTACCAGGTCATCGGCAAGAA
	R-CGTAGGTGCGGAGCTCAATT
GAPDH	F-ACACCCACTCCTCCACCTTT
	R-TAGCCAAATTCGTTGTCATACC

Caspase: Cysteine aspartate-specific protease; AIF: apoptosis-inducing factor; Endo G: endonuclease G ; GAPDH: glyceraldehyde-3-phosphate dehydrogenase. Each assay was conducted in at least triplicate to ensure reproducibility.

Western blotting analysis. Approximately 5×10^6 cells/well were treated with 50 μM GA for 0, 6, 12 and 24 h. Cells from each treatment were lysed in PRO-PREPTM protein extraction solution (iNtRON Biotechnology, Seongnam, Gyeonggi-Do, Korea). The total proteins from lysed cells were determined by using the Bio-Rad protocol as described previously (18, 22). The levels of proteins associated with G_0/G_1 phase regulation (p27, p21, cyclin E and cyclin D1/2/3) and apoptosis (fatty acid synthase (FAS), FASL, caspase-8, -9, -3, cytochrome *c*, apoptosis-inducing factor (AIF), endonuclease G (Endo G), BID, BAX, BCL-2 and caspase-4) were determined by sodium dodecylsulfate polyacrylamide gel electrophoresis (SDS-PAGE). Each sample was stained with primary antibodies (Santa Cruz Biotechnology Inc., Santa Cruz, CA, USA) and then washed twice, followed by staining by secondary antibody which was then detected by chemiluminescence (ECL kit; Millipore, Billerica, MA, USA) and autoradiography using X-ray film (17, 22).

Real-time PCR for caspase-3, -8 and -9, AIF and Endo G. The total RNA was extracted from HL-60 cells after treatment with 50 μM GA for 0, 12, 24 h by using Qiagen RNeasy Mini Kit (Qiagen, inc, Valencia, CA, USA) as described previously (13, 23). RNA samples were reverse-transcribed for 30 min at 42˚C with High Capacity cDNA Reverse Transcription Kit according to the standard protocol of the supplier (Applied Biosystems, Foster City, CA, USA). Quantitative PCR was performed using the following conditions: 2 min at 50˚C, 10 min at 95˚C, and 40 cycles of 15 s at 95˚C and 1 min at 60˚C, using 1 μl of the cDNA reverse-transcribed as described above, 2× SYBR Green PCR Master Mix (Applied Biosystems) and 200 nM of forward and reverse primers (Table I) (17-18). Each assay was run on an Applied Biosystems 7300 Real-

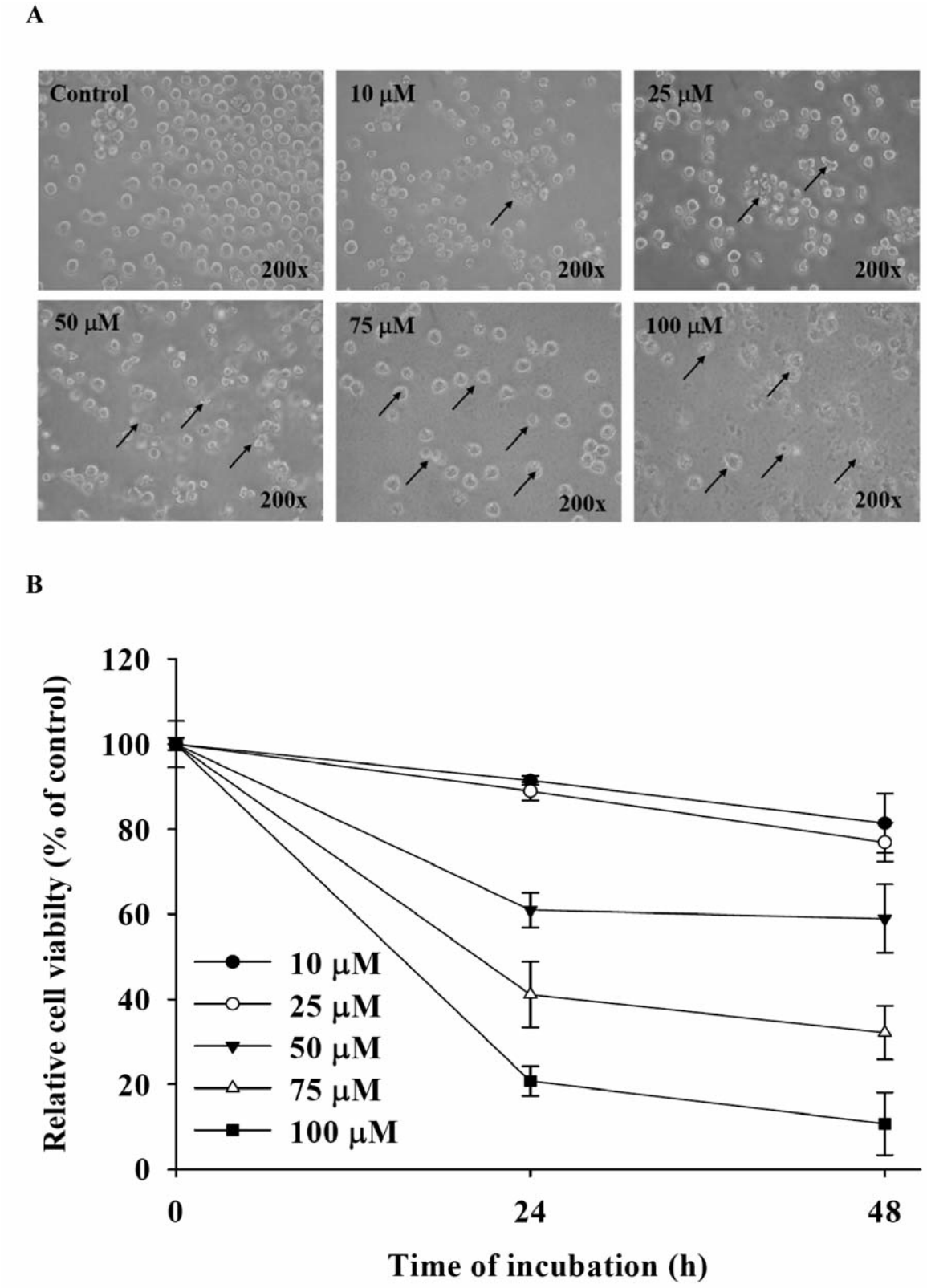

Figure 1. *GA affected cell morphological changes and the percentage of viable HL-60 cells. Cells were plated in RPMI 1640 medium + 10% FBS with 0, 10, 25, 50, 75 and 100 μM GA for 24 or 48 h. The morphological changes were examined under a phase-contrast microscope (A), and the cell viability was measured and determined by flow cytometry (B) as described in the Materials and Methods. Each point is the mean±S.D. of three experiments.*

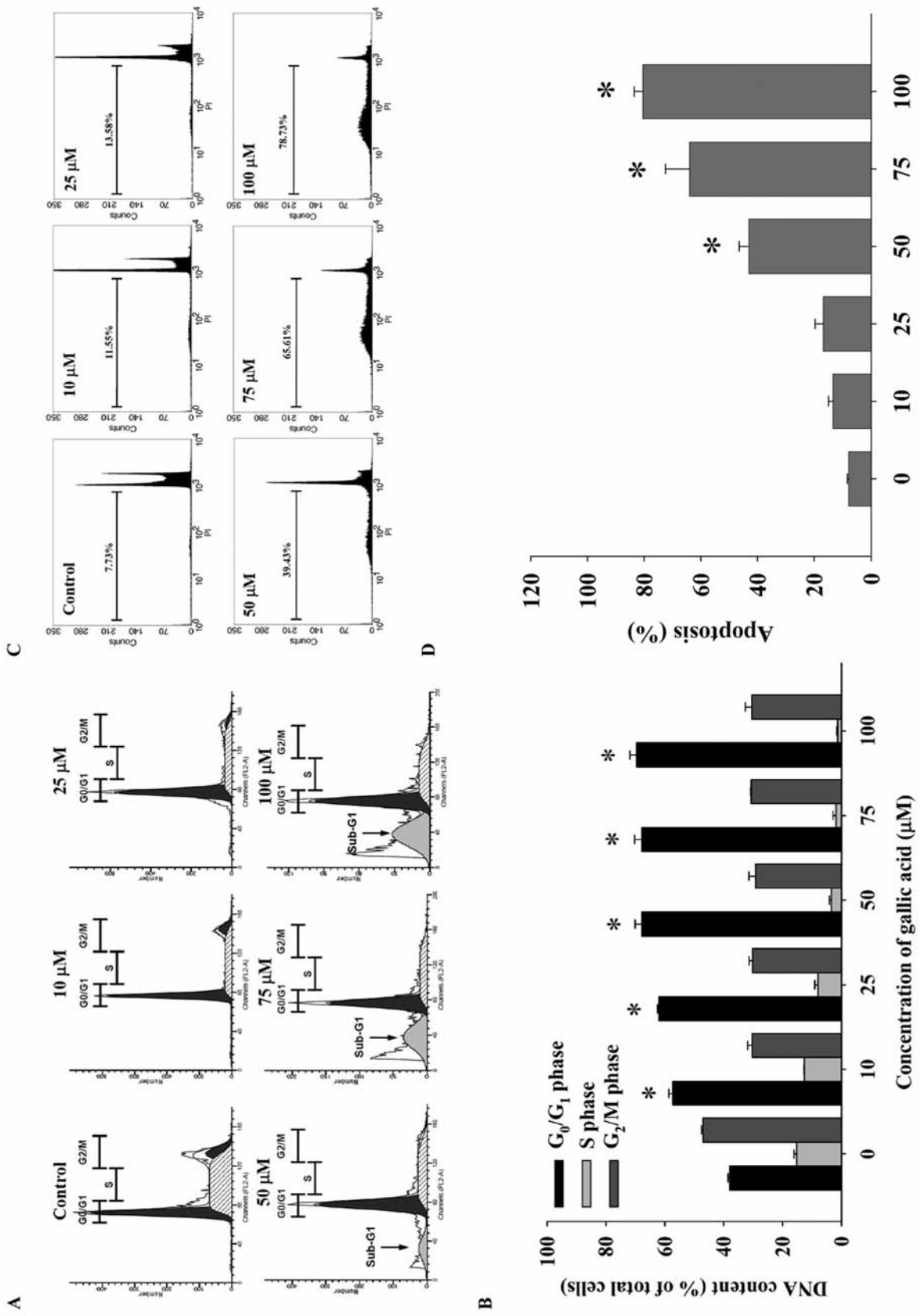

Figure 2. *GA induced G_0/G_1 phase arrest and a sub-G_1 group of HL-60 cells. Cells were plated in RPMI-1640 medium +10% FBS with 10, 25, 50, 75 and 100 μM GA for 24 h and the cells were analyzed for DNA content. A: Representative profiles for Modfit software; B: DNA content of cells in each phase (%); C: profile of sub-G1 population from BD CellQuest Pro software; D: quantification of apoptosis (%) by flow cytometry. Each point is the mean±S.D. of three experiments. *$p<0.05$, Significantly different from the control (0 μM GA).*

Time PCR system in triplicate and expression fold-changes were derived using the comparative C_T method.

Immunofluorescence staining by confocal laser scanning microscopy. Approximately 2×10^5 cells/well plated on 4-well chamber slides were treated without or with 50 μM GA for 24 h. Cells were then fixed in 4% formaldehyde (Sigma-Aldrich Corp.) in PBS for 15 min, permeabilized with 0.3% Triton X-100 in PBS for 1 h with blocking of non-specific binding sites using 2% BSA. Fixed cells were incubated with primary anti-AIF, anti-Endo G and anti-growth arrest DNA damage 153 (GADD153) (1:100 dilution) overnight and then exposed to the secondary antibody (fluorescein isothiocyanate-conjugated goat anti-mouse IgG at 1:100 dilution), followed by DNA staining with PI. Photomicrographs were obtained using a Leica TCS SP2 Confocal Spectral Microscope (13, 19).

Statistical analysis. All data were expressed as mean±S.D. from at least three separate experiments. Statistical calculations of the data were performed by one-way ANOVA followed by Dunnett's test. A *p*-value of less than 0.05 was taken as being statistically significant.

Results

Effects of GA on morphology and viability of HL-60 cells. After cells were treated with GA, morphological changes were examined after 24 h or 48 h exposure under a phase-contrast microscope and cell viability was determined by flow cytometry. Figure 1A shows that GA-induced morphological changes, cell membrane shrinkage and apoptotic bodies were observed. Figure 1B shows that viable cells decreased as time and concentration increased. This finding suggests that GA had a dose- and time-dependent cytotoxic effect on HL-60 cells.

GA-induced G_0/G_1 phase arrest and apoptosis in HL-60 cells. Cells were treated with different concentrations of GA for 24 h, and DNA content and the sub-G_1 population were examined by flow cytometry. The results showed that increased concentrations of GA led to an increase in the percentage of cells in G_0/G_1, and a decrease in G_2/M and S phases (Figure 2A and B). The data indicated GA induced G_0/G_1 phase arrest of HL-60 cells. Moreover, a sub-G_1 group (apoptotic cells) also appeared in the cell cycle distribution, suggesting that GA induced apoptosis in HL-60 cells (Figure 2A and C). After exposure to 50 μM GA, the percentage of apoptotic cells reached 39.43% in HL-60 cells. GA induced from 11.55% to 78.73% apoptosis of treated cells and these effects were dose-dependent (Figure 2D).

Effects of GA on the expressions of G_0/G_1 phase regulated proteins from HL-60 cells. Cells were treated with 50 μM GA for 6, 12 and 24 h, and we then examined the associated protein levels (p27, p21, cyclin E and cyclin D1/2/3) by Western blotting. As shown in Figure 3, the levels of p21 and p27 increased, while the levels of cyclin D1/2/3 and cyclin E decreased on treatment with GA. Based on these results, these effects might lead to G_0/G_1 phase arrest in GA-treated HL-60 cells.

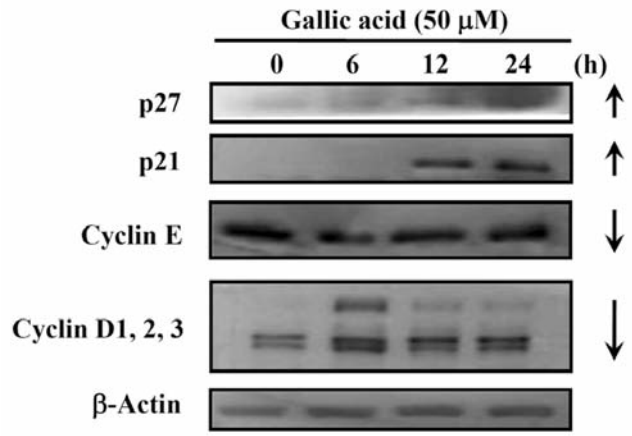

Figure 3. *GA affected the G_0/G_1 phase associated protein levels in HL-60 cells. Cells were treated with 50 μM GA for 0, 6, 12 and 24 h. Cells were harvested from each sample and G_0/G_1 phase-associated proteins were measured by Western blotting. The protein levels of p27, p21, p53, cyclin E and cyclin D1/2/3 were examined by using SDS-PAGE gel electrophoresis as described in the Materials and Methods. Anti-β-actin antibody was used as an internal control for Western blotting analysis.*

Effects of GA on chromatin condensation and DNA damage in HL-60 cells. GA-induced chromatin condensation (an apoptotic characteristic) and DNA damage were examined by DAPI staining and Comet assay, respectively. Apoptosis of treated cells was observed by DAPI staining (Figure 4A), and the results indicated that GA induced apoptosis in a dose-dependent manner (Figure 4B). The comet assay showed that higher concentrations (75 and 100 μM) of GA led to a longer DNA migration smear (comet tail) (Figure 4C) as compared to the control that did not show Comet occurrence. The results further support GA-induced DNA damage in HL-60 cells in a dose-dependent manner.

Effects of GA on $\Delta\Psi_m$, Ca^{2+} and ROS. Cells were exposed to 50 μM GA for various periods of time, and $\Delta\Psi_m$ was analyzed and quantified by flow cytometry and BD CellQuest Pro software. Results indicated that $\Delta\Psi_m$ was significantly reduced after 24-h treatment with GA (Figure 5A). When cells were treated with 50 μM GA, Ca^{2+} level significantly increased at 6, 12 and 24 h exposure (Figure 5B). Nevertheless, our results showed that GA at 50 μM did not stimulate ROS production in HL-60 cells after co-incubation for 0.5, 1, 3, 6 and 12 h (Figure 5C).

Effects of GA on the expressions of apoptosis-associated proteins in HL-60 cells. In order to characterize the molecular mechanism of GA-induced apoptosis in HL-60 cells, we examined the expressions of apoptosis-associated proteins by Western blotting. The protein levels of FAS and FASL were increased at early periods (6-12 h) (Figure 6A),

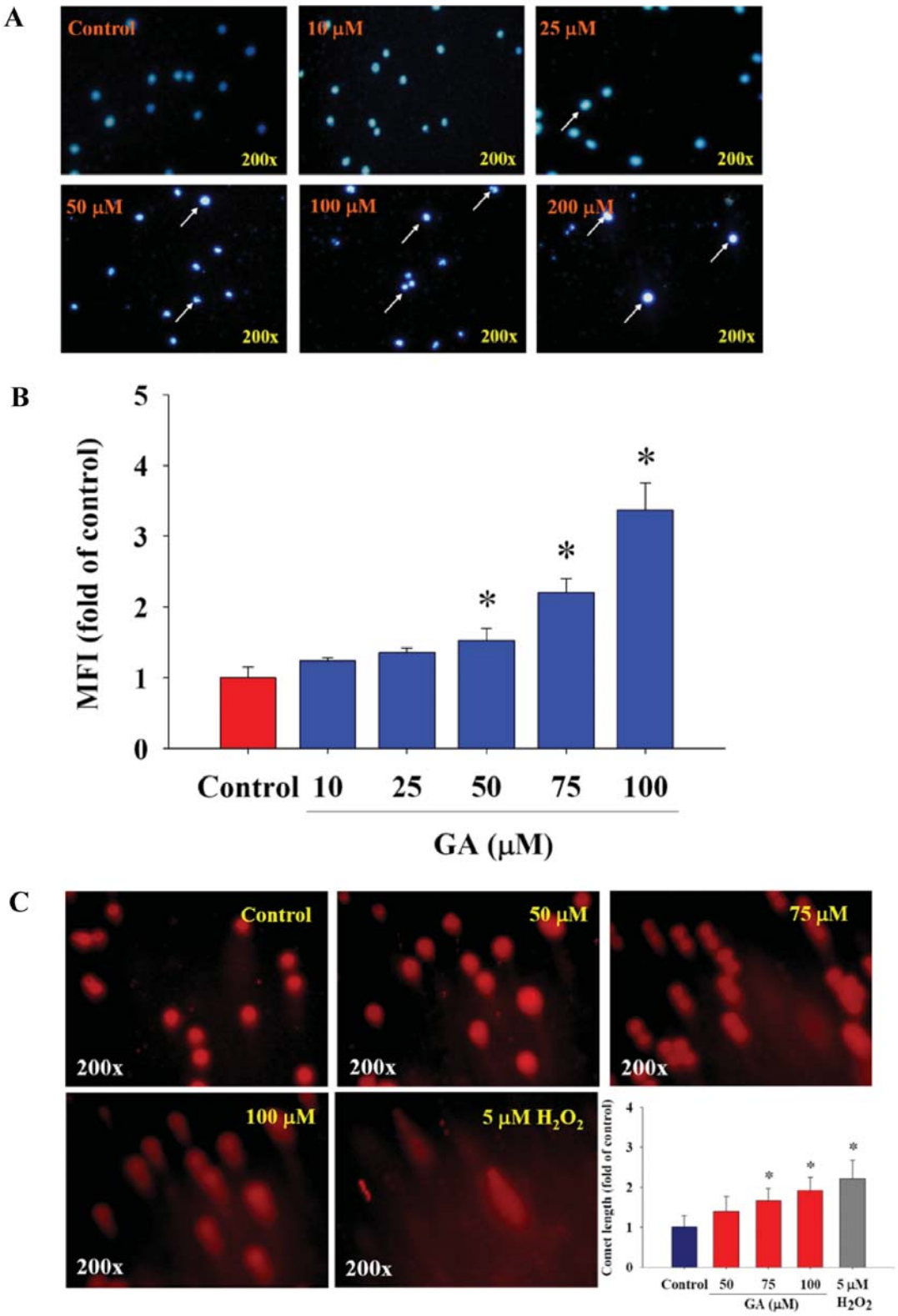

Figure 4. *GA induced apoptosis and DNA damage in HL-60 cells. Cells were incubated with 0, 10, 25, 50, 75 or 100 μM GA for 24 h. Apoptotic cells were photographed by fluorescence microscopy with DAPI staining (A) and for quantification of apoptosis (B). DNA damage was assessed by fluorescence microscopy for comet assay (C) as described in the Materials and Methods. MFI: Mean fluorescence intensity.*

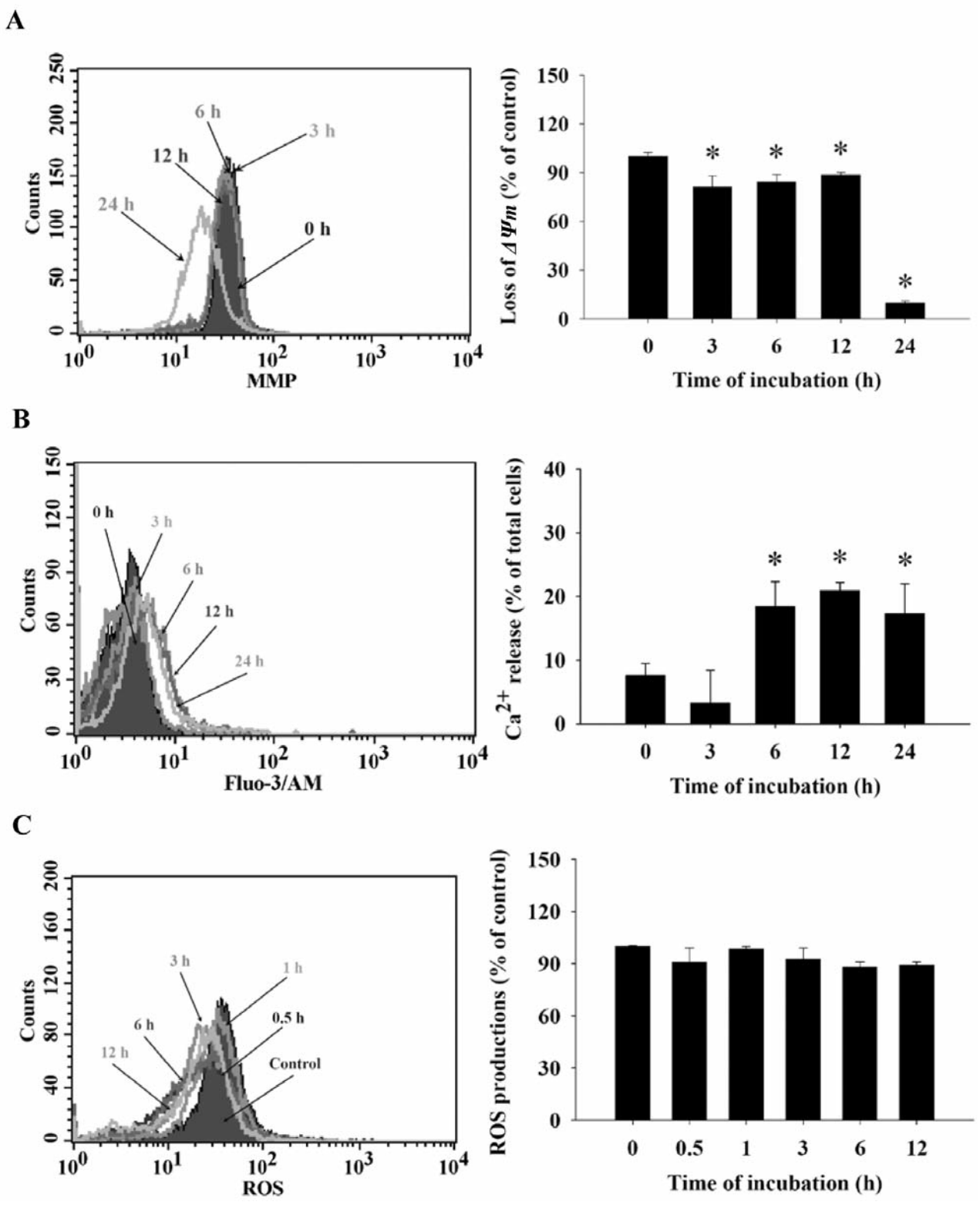

Figure 5. *Effects of GA on the levels of mitochondrial membrane potential ($\Delta\Psi_m$), intracellular Ca^{2+} and reactive oxygen species (ROS) in HL-60 cells. Cells were incubated with 50 μM GA for various time periods before being stained by $DiOC_6$ for the $\Delta\Psi_m$ levels (A), Fluo-3/AM for the intracellular Ca^{2+} levels (B), 2,7-dichlorodihydrofluorescein diacetate for ROS levels determined (C), then by flow cytometric analysis as described in the Materials and Methods. Each experiment was carried our with triple sets. *p<0.05, Significantly different from the control.*

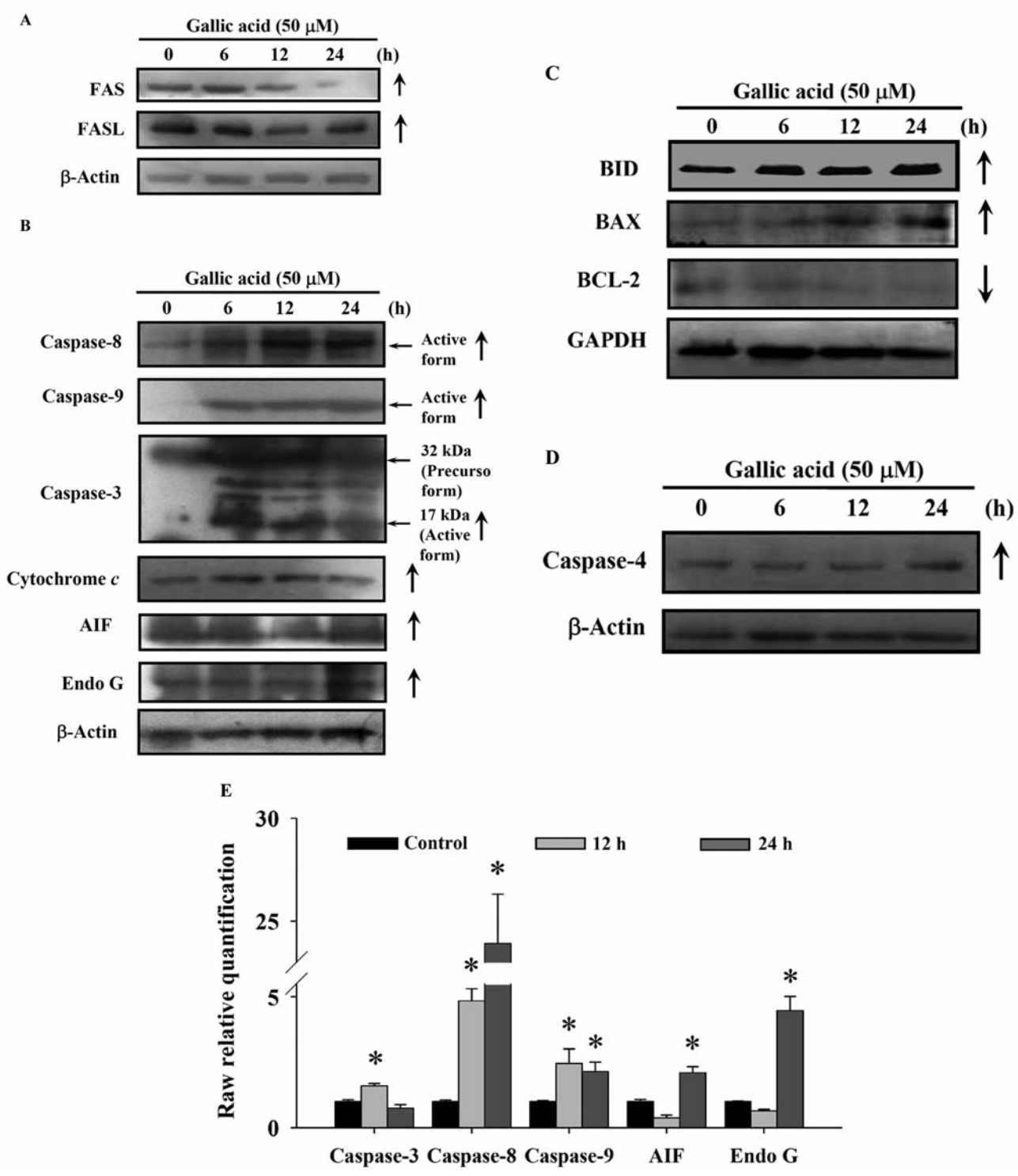

Figure 6. *GA affected protein and mRNA expression of apoptosis-related proteins in HL-60 cells. A total of 5×10^5 HL-60 cells/ml cells were treated with 50 μM GA for 0, 6, 12 and 24 h. Cells were harvested from each sample and associated proteins were measured by Western blotting. The protein levels of FAS, FASL (A); and caspase-8, caspase-9, caspase-3, cytochrome c, AIF and Endo G (B); BID, BAX, BCL-2 (C); caspase-4 protein levels were examined by using SDS-PAGE gel electrophoresis and Western blotting as described in the Materials and Methods. The total RNA was extracted from HL-60 cells after exposure to 50 μM GA for 0, 12 and 24 h and RNA samples were reverse-transcribed cDNA for real-time PCR. The expressions of caspase -3, caspase-8, caspase-9, AIF and Endo G mRNA relative to that of GAPDH presented in panel (E). Data represent the mean±S.D. of three experiments. *p< 0.05, Significantly different from the 0 h GA treatment.*

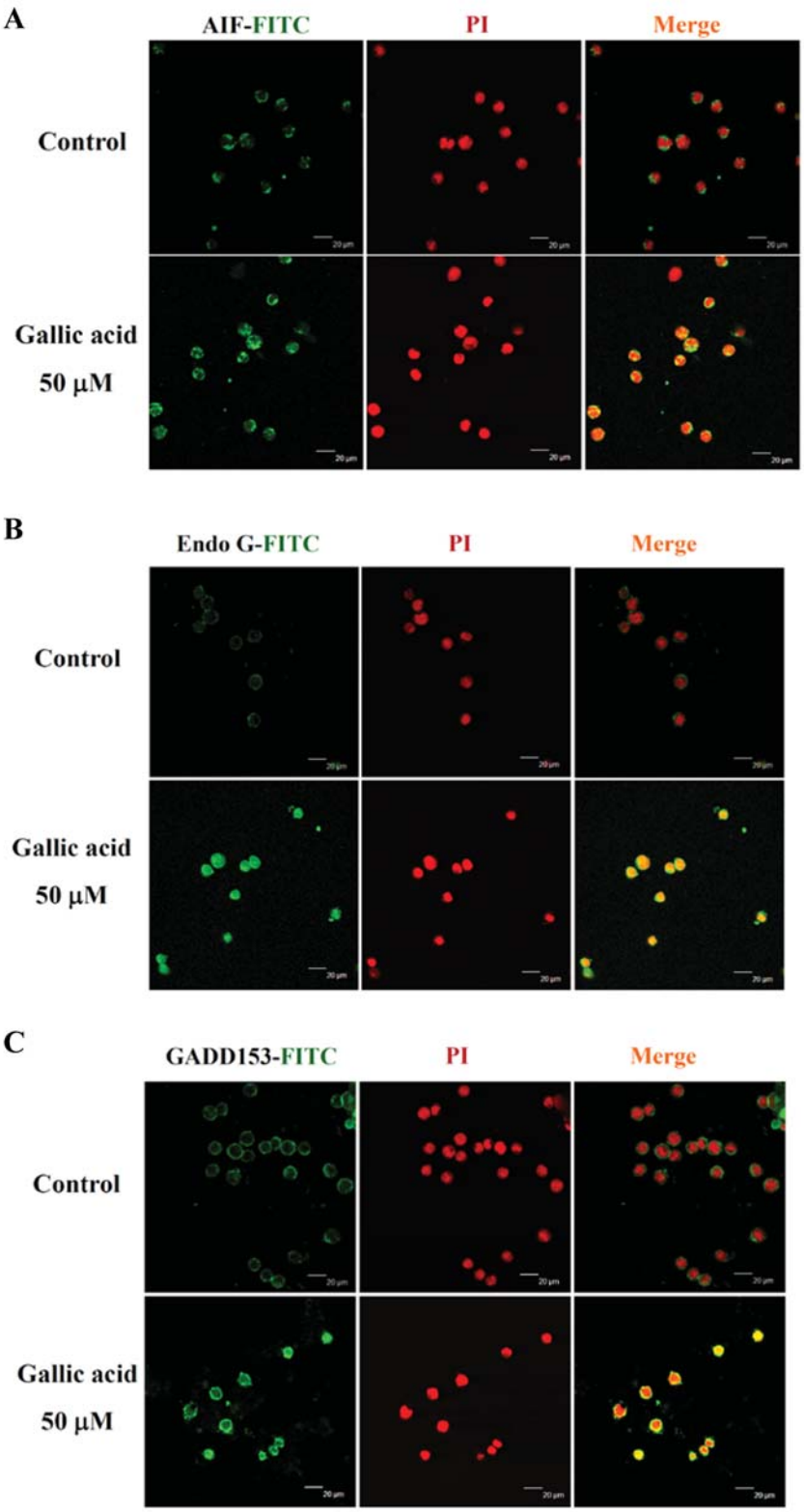

Figure 7. *GA stimulated translocation of AIF, EngoG and GADD153 proteins. HL-60 cells (5×10^4 cells/well) were plated on 4-well chamber slides and then were treated with or without 50 μM GA for 24 h, before they were stained by antibodies as described in the Material and methods. The results from confocal laser microscopy are shown A: AIF; B: Endo G; C: GADD153.*

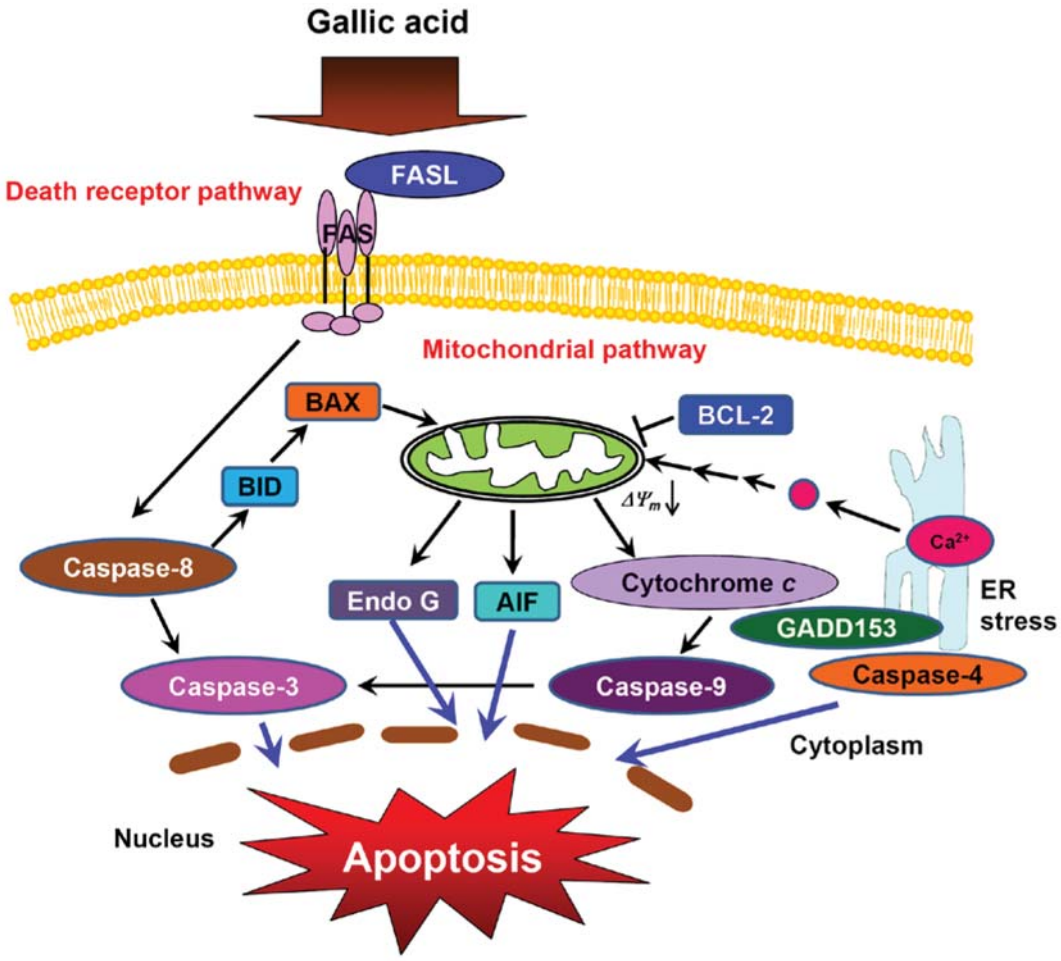

Figure 8. *The proposed molecular signaling pathways of GA-induced cell cycle arrest and apoptosis in human leukemia HL-60 cells.*

and the levels of cytochrome *c*, caspase-3, -8 and -9, AIF, Endo G (Figure 6B), BID, BAX, BCL-2 (Figure 6C), and caspase-4 (Figure 6D) were up-regulated in GA-treated HL-60 cells. Thus, these findings suggest that GA-triggered apoptotic death in HL-60 cells is mediated through caspase cascades and mitochondria-dependent pathways.

Effects of GA on the mRNA expression in HL-60 cells. Total RNA was isolated and expression of apoptosis-associated genes was examined by real-time PCR after cells were treated without or with GA for 12 and 24 h. Expression levels of caspase-3, -8 and -9, AIF and Endo G mRNA were significantly increased in GA-treated HL-60 cells, as can be seen in Figure 6E.

GA translocated protein levels of AIF, Endo G and GADD153 in HL-60 cells. As shown in Figure 7, increased levels of AIF, Endo G and GADD153 were observed after treatment with GA for 24 h. In the merged panels, it can be seen that GA promoted AIF and Endo G (Figure 7A and B) release from mitochondria and GADD153 was trafficked to nuclei in HL-60 cells (Figure 7C).

Discussion

GA, one of the components in traditional Chinese medicine 'Wen-Pi-Tang', has been used for the treatment of various diseases, including chronic renal failure (24). Much evidence supports the anticancer activity of GA in human and mouse cell lines (25-27). In the present study, we first demonstrated that GA reduced the percentage of viable leukemia HL-60 cells in a time- and dose-dependent manner (Figure 1B). We suggest that GA induced the extrinsic apoptotic pathway through FAS and the intrinsic apoptotic pathway (Figure 8). GA also induced caspase-3, -8 and -9 expression in HL-60 cells (Figure 6B). On the other hand, BCL-2 family proteins

were affected, resulting in a pro-apoptotic cell environment (Figure 6C). HL-60 cells appeared to be more sensitive to GA effects as compared with normal cells (28, 29). We suggest that GA-triggered cell death was mediated through the regulation of multiple signaling pathways, which then resulted in cell apoptosis by the mechanism as shown in Figure 8.

GA induced G_0/G_1 phase arrest in HL-60 cells inhibiting cell cycle progression at G_0/G_1 phase (Figure 2B). Cell cycle arrest in cancer cells is considered one of the most effective strategies for the control of tumor growth (30). GA also interfered with the G_2/M phase in colon adenocarcinoma cells (31), but it did not affect cell cycle in other cancer lines (5, 32). We suggest that GA-induced cell death or cell cycle arrest may differ depending on the type of cancer cell line used (33). Our results showed that GA-induced apoptosis was mainly associated with an increase the number of apoptotic cells (sub-G_1 population) which was dose-dependent (Figure 2D). Nuclear staining with DAPI confirmed the appearance of apoptotic HL-60 cells after exposure to GA (Figure 4A and B). Moreover, GA promoted intracellular Ca^{2+} release (Figure 5B) and reduced the level of $\Delta\Psi_m$ (Figure 5A), which led to the release of cytochrome *c* from mitochondria. This is agreement with a previous study, which indicated that GA induced apoptosis through generation, Ca^{2+} influx and activation of calmodulin (5).

We also investigated the role of BCL-2 family proteins in GA-induced apoptosis and found an increase in the expression of BAX protein and a decrease in the expression of BCL-2 in examined HL-60 cells (Figure 6C). An increase in the ratio of BAX/BCL-2 stimulates the release of cytochrome *c* from the mitochondria into the cytosol, promoting activation of caspase-9 which then binds to apoptotic protease activating factor-1 (APAF-1), leading to the activation of caspase-3 and poly(ADP-ribose) polymerase (PARP) (34-35). Our results showed that HL-60 cells treated with GA, had increased protein and mRNA levels of caspase-3,-8 and -9, AIF, and Endo G protein supporting the induction of the caspase cascades in GA-induced apoptosis. It was reported that agents can induce apoptosis through AIF-mediated caspase-independent mitochondrial pathway (36-38).

The possible effects of GA on cell cycle and apoptosis-related proteins and the possible mechanism of action are summarized in Figure 8. Our findings of the present study provide new perspectives for further research on toxicology and pharmacology of GA as a possible candidate for treatment of leukemia.

Acknowledgements

This work was supported by a grant from Taiwan Department of Health China Medical University Hospital Cancer Research Center of Excellence (DOH100-TD-C-111-005).

References

1 Fiuza SM, Gomes C, Teixeira LJ, Girao da Cruz MT, Cordeiro MN, Milhazes N, Borges F and Marques MP: Phenolic acid derivatives with potential anticancer properties – a structure-activity relationship study. Part 1: methyl, propyl and octyl esters of caffeic and gallic acids. Bioorg Med Chem *12*: 3581-3589, 2004.

2 Grundhofer P, Niemetz R, Schilling G and Gross GG: Biosynthesis and subcellular distribution of hydrolyzable tannins. Phytochemistry *57*: 915-927, 2001.

3 Manna SK, Kuo MT and Aggarwal BB: Overexpression of gamma-glutamylcysteine synthetase suppresses tumor necrosis factor-induced apoptosis and activation of nuclear transcription factor-kappa B and activator protein-1. Oncogene *18*: 4371-4382, 1999.

4 Klein E and Weber N: *In vitro* test for the effectiveness of antioxidants as inhibitors of thiyl radical-induced reactions with unsaturated fatty acids. J Agric Food Chem *49*: 1224-1227, 2001.

5 Inoue M, Suzuki R, Koide T, Sakaguchi N, Ogihara Y and Yabu Y: Antioxidant, gallic acid, induces apoptosis in HL-60RG cells. Biochem Biophys Res Commun *204*: 898-904, 1994.

6 Ji BC, Hsu WH, Yang JS, Hsia TC, Lu CC, Chiang JH, Yang JL, Lin CH, Lin JJ, Wu Suen LJ, Wood WG and Chung JG: Gallic acid induces apoptosis *via* caspase-3 and mitochondrion-dependent pathways *in vitro* and suppresses lung xenograft tumor growth *in vivo*. J Agric Food Chem *57*: 7596-7604, 2009.

7 Yoshioka K, Kataoka T, Hayashi T, Hasegawa M, Ishi Y and Hibasami H: Induction of apoptosis by gallic acid in human stomach cancer KATO III and colon adenocarcinoma COLO 205 cell lines. Oncol Rep *7*: 1221-1223, 2000.

8 Kang MK, Kang NJ, Jang YJ, Lee KW and Lee HJ: Gallic acid induces neuronal cell death through activation of c-Jun N-terminal kinase and down-regulation of Bcl-2. Ann NY Acad Sci *1171*: 514-520, 2009.

9 Sakaguchi N, Inoue M and Ogihara Y: Reactive oxygen species and intracellular Ca^{2+}, common signals for apoptosis induced by gallic acid. Biochem Pharmacol *55*: 1973-1981, 1998.

10 Ban JY, Nguyen HT, Lee HJ, Cho SO, Ju HS, Kim JY, Bae K, Song KS and Seong YH: Neuroprotective properties of gallic acid from Sanguisorbae radix on amyloid beta protein (25-35)-induced toxicity in cultured rat cortical neurons. Biol Pharm Bull *31*: 149-153, 2008.

11 Kawada M, Ohno Y, Ri Y, Ikoma T, Yuugetu H, Asai T, Watanabe M, Yasuda N, Akao S, Takemura G, Minatoguchi S, Gotoh K, Fujiwara H and Fukuda K: Anti-tumor effect of gallic acid on LL-2 lung cancer cells transplanted in mice. Anticancer Drugs *12*: 847-852, 2001.

12 Lo C, Lai TY, Yang JH, Yang JS, Ma YS, Weng SW, Chen YY, Lin JG and Chung JG: Gallic acid induces apoptosis in A375.S2 human melanoma cells through caspase-dependent and -independent pathways. Int J Oncol *37*: 377-385, 2010.

13 Lu CC, Yang JS, Huang AC, Hsia TC, Chou ST, Kuo CL, Lu HF, Lee TH, Wood WG and Chung JG: Chrysophanol induces necrosis through the production of ROS and alteration of ATP levels in J5 human liver cancer cells. Mol Nutr Food Res *54*: 967-976, 2010.

14 Wu SH, Hang LW, Yang JS, Chen HY, Lin HY, Chiang JH, Lu CC, Yang JL, Lai TY, Ko YC and Chung JG: Curcumin induces apoptosis in human non-small cell lung cancer NCI-H460 cells through ER stress and caspase cascade- and mitochondria-dependent pathways. Anticancer Res *30*: 2125-2133, 2010.

15 Kuo JH, Chu YL, Yang JS, Lin JP, Lai KC, Kuo HM, Hsia TC and Chung JG: Cantharidin induces apoptosis in human bladder cancer TSGH 8301 cells through mitochondria-dependent signal pathways. Int J Oncol *37*: 1243-1250, 2010.

16 Yang JS, Hour MJ, Huang WW, Lin KL, Kuo SC and Chung JG: MJ-29 inhibits tubulin polymerization, induces mitotic arrest, and triggers apoptosis *via* cyclin-dependent kinase 1-mediated Bcl-2 phosphorylation in human leukemia U937 cells. J Pharmacol Exp Ther *334*: 477-488, 2010.

17 Yu FS, Yang JS, Yu CS, Lu CC, Chiang JH, Lin CW and Chung JG: Safrole induces apoptosis in human oral cancer HSC-3 cells. J Dent Res *90*: 168-174, 2011.

18 Chiang JH, Yang JS, Ma CY, Yang MD, Huang HY, Hsia TC, Kuo HM, Wu PP, Lee TH and Chung JG: Danthron, an anthraquinone derivative, induces DNA damage and caspase cascades-mediated apoptosis in SNU-1 human gastric cancer cells through mitochondrial permeability transition pores and Bax-triggered pathways. Chem Res Toxicol *24*: 20-29, 2011.

19 Chen JC, Lu KW, Tsai ML, Hsu SC, Kuo CL, Yang JS, Hsia TC, Yu CS, Chou ST, Kao MC, Chung JG and Wood WG: Gypenosides induced G0/G1 arrest *via* CHk2 and apoptosis through endoplasmic reticulum stress and mitochondria-dependent pathways in human tongue cancer SCC-4 cells. Oral Oncol *45*: 273-283, 2009.

20 Lee JH, Li YC, Ip SW, Hsu SC, Chang NW, Tang NY, Yu CS, Chou ST, Lin SS, Lino CC, Yang JS and Chung JG: The role of Ca^{2+} in baicalein-induced apoptosis in human breast MDA-MB-231 cancer cells through mitochondria- and caspase-3-dependent pathway. Anticancer Res *28*: 1701-1711, 2008.

21 Lin CC, Kuo CL, Lee MH, Lai KC, Lin JP, Yang JS, Yu CS, Lu CC, Chiang JH, Chueh FS and Chung JG: Wogonin triggers apoptosis in human osteosarcoma U-2 OS cells through the endoplasmic reticulum stress, mitochondrial dysfunction and caspase-3-dependent signaling pathways. Int J Oncol *39*: 217-224, 2011.

22 Ji BC, Hsu WH, Yang JS, Hsia TC, Lu CC, Chiang JH, Yang JL, Lin CH, Lin JJ, Suen LJ, Gibson Wood W and Chung JG: Gallic acid induces apoptosis *via* caspase-3 and mitochondrion-dependent pathways *in vitro* and suppresses lung xenograft tumor growth *in vivo*. J Agric Food Chem *57*: 7596-7604, 2009.

23 Hsia TC, Chung JG, Lu HF, Ho HC, Yang CC, Lu KH and Hung CF: The effect of paclitaxel on 2-aminofluorene-DNA adducts formation and arylamine N-acetyltransferase activity and gene expression in human lung tumor cells (A549). Food Chem Toxicol *40*: 697-703, 2002.

24 Rhyu DY, Kang KS, Sekiya M, Tanaka T, Park JC and Yokozawa T: Active compounds isolated from traditional Chinese prescription Wen-Pi-Tang protecting against peroxynitrite-induced LLC-PK(1) cell damage. Am J Chin Med *36*: 761-770, 2008.

25 Kanai S and Okano H: Mechanism of the protective effects of sumac gall extract and gallic acid on the progression of CCl4-induced acute liver injury in rats. Am J Chin Med *26*: 333-341, 1998.

26 Agarwal C, Tyagi A and Agarwal R: Gallic acid causes inactivating phosphorylation of cdc25A/cdc25C-cdc2 *via* ATM-Chk2 activation, leading to cell cycle arrest, and induces apoptosis in human prostate carcinoma DU145 cells. Mol Cancer Ther *5*: 3294-3302, 2006.

27 Sakagami H, Yokote Y and Akahane K: Changes in amino acid pool and utilization during apoptosis in HL-60 cells induced by epigallocatechin gallate or gallic acid. Anticancer Res *21*: 2441-2447, 2001.

28 Ye X, Krohn RL, Liu W, Joshi SS, Kuszynski CA, McGinn TR, Bagchi M, Preuss HG, Stohs SJ and Bagchi D: The cytotoxic effects of a novel IH636 grape seed proanthocyanidin extract on cultured human cancer cells. Mol Cell Biochem *196*: 99-108, 1999.

29 Inoue M, Suzuki R, Sakaguchi N, Li Z, Takeda T, Ogihara Y, Jiang BY and Chen Y: Selective induction of cell death in cancer cells by gallic acid. Biol Pharm Bull *18*: 1526-1530, 1995.

30 Nam W, Tak J, Ryu JK, Jung M, Yook JI, Kim HJ and Cha IH: Effects of artemisinin and its derivatives on growth inhibition and apoptosis of oral cancer cells. Head Neck *29*: 335-340, 2007.

31 Salucci M, Stivala LA, Maiani G, Bugianesi R and Vannini V: Flavonoids uptake and their effect on cell cycle of human colon adenocarcinoma cells (Caco2). Br J Cancer *86*: 1645-1651, 2002.

32 Hsu CL, Huang SL and Yen GC: Inhibitory effect of phenolic acids on the proliferation of 3T3-L1 preadipocytes in relation to their antioxidant activity. J Agric Food Chem *54*: 4191-4197, 2006.

33 Serrano A, Palacios C, Roy G, Cespon C, Villar ML, Nocito M and Gonzalez-Porque P: Derivatives of gallic acid induce apoptosis in tumoral cell lines and inhibit lymphocyte proliferation. Arch Biochem Biophys *350*: 49-54, 1998.

34 Bossy-Wetzel E and Green DR: Caspases induce cytochrome c release from mitochondria by activating cytosolic factors. J Biol Chem *274*: 17484-17490, 1999.

35 Pandey P, Saleh A, Nakazawa A, Kumar S, Srinivasula SM, Kumar V, Weichselbaum R, Nalin C, Alnemri ES, Kufe D and Kharbanda S: Negative regulation of cytochrome c-mediated oligomerization of Apaf-1 and activation of procaspase-9 by heat shock protein 90. EMBO J *19*: 4310-4322, 2000.

36 Wang Y, He QY, Sun RW, Che CM and Chiu JF: GoldIII porphyrin 1a induced apoptosis by mitochondrial death pathways related to reactive oxygen species. Cancer Res *65*: 11553-11564, 2005.

37 Liu KC, Huang YT, Wu PP, Ji BC, Yang JS, Yang JL, Chiu TH, Chueh FS and Chung JG: The roles of AIF and Endo G in the apoptotic effects of benzyl isothiocyanate on DU 145 human prostate cancer cells *via* the mitochondrial signaling pathway. Int J Oncol *38*: 787-796, 2011.

38 Zhang W, Wang Z and Chen T: Curcumol induces apoptosis *via* caspases-independent mitochondrial pathway in human lung adenocarcinoma ASTC-a-1 cells. Med Oncol *28*: 307-314, 2011.

Received April 3, 2011
Revised May 24, 2011
Accepted May 26, 2011